UC Davis
UC Davis Previously Published Works

Title

Effects of Climate Variability on Snowmelt and Implications for Organic Matter in a High-Elevation Lake

Permalink

Journal

ISSN

Authors

Sadro, Steven
Sickman, James O
Melack, John M
et al.

Publication Date

DOI

Peer reviewed

Key Points:
- The magnitude and water content of winter snowpack explain the majority of variation in timing and rate of snowmelt
- Catchment snowpack controls interannual variation in phytoplankton biomass by regulating nutrients, water temperature, and flushing rates
- High interannual variation in mountain snowfall may mask weak long-term climate-related changes in phytoplankton biomass

Correspondence to:
S. Sadro,
ssadro@ucdavis.edu

Effects of Climate Variability on Snowmelt and Implications for Organic Matter in a High-Elevation Lake

Steven Sadro[1] [iD], James O. Sickman[2], John M. Melack[3], and Kevin Skeen[2]

[1]Department of Environmental Science and Policy, University of California, Davis, CA, USA, [2]Department of Environmental Science, University of California, Riverside, CA, USA, [3]Earth Research Institute, University of California, Santa Barbara, CA, USA

Abstract Few coupled lake-watershed studies examine long-term effects of climate on the ecosystem function of lakes in a hydrological context. We use 32 years of hydrological and biogeochemical data from a high-elevation site in the Sierra Nevada of California to characterize variation in snowmelt in relation to climate variability and explore the impact on factors affecting phytoplankton biomass. The magnitude of accumulated winter snow, quantified through basinwide estimates of snow water equivalent (SWE), was the most important climate factor controlling variation in the timing and rate of spring snowmelt. Variations in SWE and snowmelt led to significant differences in lake flushing rate, water temperature, and nitrate concentrations across years. On average in dry years, snowmelt started 25 days earlier and proceeded 7 mm/day slower, and the lake began the ice-free season with nitrate concentrations ~2 μM higher and water temperatures 9°C warmer than in wet years. Flushing rates in wet years were 2.5 times larger than those in dry years. Consequently, particulate organic matter concentrations, a proxy for phytoplankton biomass, were 5–6 μM higher in dry years. There was a temporal trend of increase in particulate organic matter across dry years that corresponded to lake warming independent of variation in SWE. These results suggest that phytoplankton biomass is increasing as a result of both interannual variability in precipitation and long-term warming trends. Our study underscores the need to account for local-scale catchment variability that may affect the accumulation of winter snowpack when predicting climate responses in lakes.

1. Introduction

Climate regulates fundamental aspects of lake ecosystem function by affecting physical, chemical, and ecological dynamics (Adrian et al., 2009; Greig et al., 2012; Kirillin, 2010). Understanding how long-term variation in climate affects the productivity of lakes remains a critical research goal (Carpenter et al., 1992; Yvon-Durocher et al., 2010). Lakes in mountain regions may be particularly sensitive to ongoing changes in climate in part because high-elevation ecosystems are warming at among the fastest rates found globally (N. Pepin et al., 2015; N. C. Pepin & Lundquist, 2008; Wang et al., 2014). While long-term studies of lake responses to climate variation in mountain systems remain somewhat limited, there is evidence of increasing algal productivity (Miller & McKnight, 2015; Park et al., 2004; Preston et al., 2016; Strub et al., 1985). However, the specific mechanisms through which climate is affecting phytoplankton remain unclear.

In particular, the combined effects of changes in temperature and hydrology are rarely considered. Because many high-elevation ecosystems have snowmelt dominated hydrology, the extent to which climate related changes alter aquatic ecosystem function is coupled to the accumulation and subsequent melt of the snowpack (Fountain et al., 2012; Jones, 2001). However, the extent to which snowmelt is changing, the factors responsible for such changes, and importantly, the implications for downstream lentic ecosystems remain unclear, especially in headwater catchments where responses may differ markedly from sites at lower elevations (Lundquist et al., 2004).

Snowpack and rates of snowmelt influence a number of factors that may directly or indirectly regulate algal productivity and biomass. Snowpack is correlated with nutrient loading rates and availability in lakes (Leydecker et al., 2001; Sebestyen et al., 2008; Sickman, Leydecker, Chang, et al., 2003; Sickman et al., 2001), In years with large snowpack, total nutrient loads are higher, but dilution during the descending limb of the hydrograph resulting from discharge-concentration hysteresis may reduce in-lake nutrient concentrations at the start of the ice-free season. The effect of snowpack on lake temperature is more direct. In years with less snow, lakes become ice-free earlier and warm more than in years with large snowpack (Preston

et al., 2016; Roberts et al., 2017). The importance of water temperature, light levels, and nutrient concentrations for phytoplankton productivity (Fee, 1980) suggests that climate and resulting snowmelt characteristics should together exert considerable bottom up control of phytoplankton biomass. Moreover, snowpack and melt rates (MRs) also directly influence water residence times in lakes. As many mountain lakes can be small, flushing rates are an important determinant of algal biomass (Sadro & Melack, 2012). While a growing number of climate analyses predict an earlier onset of melt (Cayan et al., 2001; Maurer et al., 2007; Preston et al., 2016), the response of snowmelt to warming may be more complex than large-scale models reflect (Lundquist et al., 2005, 2009). Disentangling their effects in mountain systems where interannual variability is high requires multiple decades of data (Goldman et al., 1989; Jassby et al., 1990; Park et al., 2004).

We use long-term hydrological and biogeochemical data from the Emerald Lake watershed in the Sierra Nevada of California to characterize variation in snowmelt characteristics in relation to interannual variation in meteorological conditions and examine subsequent effects on variation in particulate organic matter (POM) as proxy for phytoplankton biomass. Winter precipitation has varied over an order of magnitude, and summer air temperatures have warmed by 2.7°C in the Emerald catchment from 1983 to 2016, providing a large gradient over which to examine responses. In this analysis we ask the following questions: (1) what climate factors govern the timing, duration, and rate of snowmelt in this small, headwater catchment? (2) Has the timing, onset, or length of snowmelt changed from 1983 to 2016? and (3) Do such changes affect phytoplankton biomass? More specifically, we hypothesize that the magnitude of accumulated winter snowpack, measured as snow water equivalent (SWE), would be the most important factor regulating hydrological characteristics during snowmelt, such that in dry years with shallower snowpack snowmelt would begin earlier and take fewer days to reach completion despite overall slower rates of melt. Similarly, we hypothesize that SWE will explain the majority of interannual variation in summer phytoplankton biomass within Emerald Lake. We predict that phytoplankton biomass will be higher in dry years than in wet years because of differences in the timing of ice-off and rates of snowmelt, and their subsequent effects on lake flushing rates, water temperature, and nutrient availability. Finally, we hypothesize that large interannual variation in SWE will mask long-term trends in phytoplankton biomass, but expect a pattern of increase associated with warming trends to occur across dry years.

2. Materials and Methods

2.1. Site Description

Emerald Lake (36°35′49″N, 118°40′29″W) is located in Sequoia National Park in the southern Sierra Nevada of California. The headwater cirque lake has a characteristic glacial carved morphometry, a 2.7 ha surface area, and 10 m maximum depth, with a volume of 16.2×10^4 m^3. The lake is oligotrophic and the attenuation coefficient for photosynthetically active radiation typically ranges from 0.2 m^{-1} to 0.3 m^{-1}. Mean summer concentration of nitrate + nitrite is 2.9 μM, and soluble reactive phosphorus (SRP) is below 0.05 μM. In general, Emerald Lake is representative of thousands of small lakes found throughout the Sierra (Melack & Stoddard, 1991). The lake and catchment have been studied for over 30 years and the biogeochemistry, hydrology, and ecosystem processes are well characterized (Melack & Stoddard, 1991; Sadro et al., 2011; Sickman, Leydecker, Chang, et al., 2003; Sickman, Melack, & Clow, 2003).

2.2. Hydrological and Meteorological Sampling

The Emerald Lake watershed is a 120 ha catchment underlain by granitic rock. It lacks significant groundwater storage or leakage, so the water balance includes inputs from snow and rain and outputs via evapotranspiration and outflow discharge (Kattelmann & Elder, 1991). Runoff from the catchment flows into the lake via four major inflows and other smaller channels and exits the lake in a single-outlet stream channel. Catchment discharge (water years 1984–2016) was computed from a continuous record of stage recorded by vented pressure transducers, installed on the outlet stream bottom, and digitally recorded on dataloggers. Pressure transducer measurements were calibrated against a staff gauge bolted to bedrock in the stream. Linear regressions were developed from periodic manual measurements of staff depth (centimeters) and transducer output (volts). The linear regressions were used to convert the continuous record of hourly voltage into mean hourly stage. The stage record was then converted into discharge units (m^3/s) using a rating curve derived from either (i) in situ measurements of discharge (i.e., salt

dilution: water years 1984–1990) or (ii) the geometry of a v-notch weir (Herschy, 1978) installed in the outlet channel to Emerald Lake (water years 1991–present). Salt dilutions involved repeated additions of salt tracer to the outlet stream and measurement of the conductivity response to compute instantaneous discharge (Kilpatrick & Cobb, 1987). The weir installed in the outlet stream is approximately 2 m wide, has a v-notch with an angle of 120° that accommodates flows of up to 0.35 m/s and two successive rectangular sections each approximately 30 cm deep designed to accommodate high and flood stage flows, up to 1 m/s and 3 m/s, respectively. The uncertainty of annual discharge based on rating curves made with salt dilutions is between ±10 and 20%, while annual discharge made with the weir during low to typical high flows is about ±4% (Sickman et al., 2001).

Meteorological data were collected at a station 30 m from the lake shore: air temperature and relative humidity were measured using a Vaisala ES 120 sensor, wind speed using a R.M. Young propeller anemometer (1.0 m/s threshold; ±0.3 m/s accuracy), downwelling shortwave radiation (285–2,800 nm) using an Eppley Precision Spectral Pyranometer, and downwelling longwave radiation (3.5 to 50 μm) using an Eppley Precision Infrared Pyrgeometer. All parameters were measured at 10-s intervals and recorded as 5-min averages except wind speed, which was recorded as hourly averages.

Nonwinter precipitation was measured with a tipping bucket rain gauge. Prior to 2000, the gauge was installed on the ground and equipped with an Alter-shield; this gauge was typically deployed from June to October and taken down before November. Starting in 2000, the gauge was attached to the tower holding the other meteorological sensors and was installed, year-round. Precipitation during the months of April, May, and November was measured in a variety of ways. Snowboards were sometimes used to sample small snowstorms during April and May. Large spring storms were sampled by digging snowpits and sampling the fresh snow. When snowboard or snowpit data were unavailable, Emerald Lake precipitation was estimated by directly using daily precipitation totals recorded at the Lodgepole Ranger Station, located at the mouth of the Tokopah Valley (5 km west of Emerald Lake, at an elevation of 2,050 m). We estimate that the uncertainty of nonwinter precipitation during water years 1984–1997 (ground-based, shield rain gauge) was ±9%, and from water years 1998–2016 the uncertainty is ±15% owing to the error introduced by the tower-mounted gauge and reliance on extrapolations from the Lodgepole Ranger Station.

2.3. Characterizing Snowpack and Snowmelt

Accumulated winter precipitation was measured by snowpack surveys conducted in late March or early-to-middle April of each year. Winters in the alpine and subalpine zones of the Sierra Nevada are sufficiently cold that little wintertime snowmelt has historically occurred, except in the case of infrequent rain-on-snow events. In addition, measurements of winter evaporation and sublimation indicate little loss of water from the snowpack (Leydecker & Melack, 2000). Thus, catchment-wide winter snowfall was estimated from snow depth surveys and measurements of snow density conducted at the time of maximum snowpack accumulation in the spring which usually occurred at the end of March or early April. Typically two to four transects starting at the lake shore and running to the edge of the catchment were measured. Transects were designed to be representative of the basin's topography including all categories of slopes, aspects, and elevations. Along transects, depths were measured with aluminum probes (graduated in centimeters) at intervals of 20 to 50 m. At each location, from three to five individual measurements were made within a 2- to 10-m circle. Snow density was primarily determined in snowpits dug and sampled during the spring snow survey. Snow density was measured in a vertical profile at 10-cm intervals using a wedge-shaped (volume = 1,000 cm^3), stainless steel cutter, and portable electronic balance. Values for each 10-cm interval were averaged to obtain a mean density for the pit. During some years, additional snow density measurements were made with a Federal-type snow sampler. Average catchment SWE was estimated by multiplying basin-mean density by mean depth and correcting for snow-free areas. The percentage of snow-free area in each watershed was obtained from aerial photographs or satellite images of the watershed taken on or near the date of the spring surveys. The estimated uncertainty of catchment SWE is ±5–10% (Sickman et al., 2001).

Across all study years, SWE and nonwinter precipitation accounted for 86% and 14% of total inputs, respectively. Evaporation and discharge accounted for 29% and 71% of outputs, respectively. Estimates of SWE were larger than measurements of discharge in all but 6 years, and on average, total inputs were 2.9% larger than total outputs. Thus, our catchment water balances appear to be unbiased and to have sufficient accuracy that long-term changes in discharge and SWE can be reliably detected.

Table 1
Descriptive Statistics for Snowmelt Characteristics Associated With Timing, Duration, and Rate of Melt

		Measure	Mean	Minimum	Maximum	Range
Timing	Start DOY	Day of water year	188	149	240	91
	Peak DOY	Day of water year	244	203	293	90
	50% DOY	Day of water year	242	206	279	73
	End DOY	Day of water year	304	257	359	102
Duration	DRL	Number of days	89	16	234	218
	DDL	Number of days	71	40	152	112
	DSM	Number of days	115	63	163	100
Rate	MRRL	mm/day	6.1	0.9	18.3	17.5
	MRDL	mm/day	6.9	1.4	13.8	12.5
	MRSM	mm/day	6.3	1.1	14.6	13.5

Note. DOY is day of the water year. Start, Peak, 50%, and End all identify the DOY on which snowmelt starts, peaks, reaches 50% cumulative discharge, and ends. The duration of melt is quantified for the entire snowmelt period (DSM) and for the rising (DRL) and descending (DDL) limbs of the hydrograph. Likewise, the rate of melt is computed for the entire snowmelt period (MRSM) and for the rising (MRRL) and descending (MRDL) of the hydrograph.

We quantified a number of specific attributes of snowmelt (Table 1). The day of the water year (DOY, starting 1 October) on which snowmelt began (Start DOY) and ended (End DOY) was quantified as the day on which cumulative discharge reached 8% and 99%, respectively. Peak snowmelt was defined as the day on which Q maximum was reached during the spring melt pulse (Max DOY). The date cumulative Q reached 50% (50% DOY) was used to characterize the center of mass for the snowmelt pulse. The duration of the rising limb (DRL), descending limb (DDL), and entire snowmelt pulse (DSM) were computed as the difference between Max DOY and 8% cumulative discharge DOY, 99% cumulative discharge DOY and Max DOY, and 99% cumulative discharge DOY and 8% cumulative discharge DOY, respectively. Annual Q was computed by summing Q for the entire water year. MR was quantified for monthly rates of discharge, and rates of discharge during the rising and falling limbs of the hydrograph. MRs were computed by summing daily discharge during the period and dividing by the corresponding number of days for the entire snowmelt period (MRSM), and during the rising limb (MRRL) and descending limb of the hydrograph (MRDL). We used exponential models to compute the rate of change in discharge during the rising and falling limbs of the hydrograph. The percent lake volume per day flushing rate was computed by dividing the volume of the snowmelt discharge pulse by the volume of the lake expressed as a percent and dividing by DSM.

2.4. Biogeochemical Sampling and Analysis

Nitrate and POM concentrations were determined for both lake and outlet steam water samples. The outlet stream was sampled at 1- to 3-day intervals during the spring using an ISCO autosampler and as grab samples during other seasons. The lake was sampled over the deepest location at depth intervals of 1, 4, 7, and 9 m. Samples were filtered at the time of collection, nitrate (~200 mL) through 1.0 μm polycarbonate membrane filters (Nuclepore) and POM samples (~500 mL) retained on precombusted (500°C for 2 hr to remove organic matter) Whatman GF/F (0.7 μm nominal) filters. While nitrate and particulate concentrations from lake samples are volume-weighted means, outlet samples generally reflect upper mixed layer values for the lake. Nitrate samples were stored in the dark at 5°C until analyzed by ion chromatography (Dionex) or colorimetrically using the cadmium reduction (EPA Method 353.2). POM samples were stored frozen at −20°C until analyzed by high-temperature combustion in an elemental analyzer. Filter blanks were routinely analyzed for C and N after rinsing with a volume of deionized water equal to the volume of sample water being filtered, and no carbon or nitrogen was detected. We computed the ambient concentration of C and N using the ambient volume of water filtered for each sample (μmoles/L). POM can be used as a proxy for phytoplankton biomass in high-elevation lakes where terrestrial particulate matter inputs are generally low. In Emerald Lake, the isotopic signature of $\delta^{13}C$, $\Delta^{14}C$, and δ^2H in POM is indistinguishable from in situ phytoplankton cultures and nutrient stoichiometry in POM reflects ranges expected for phytoplankton (e.g., Figure 5c).

2.5. Statistical Analyses

We used analysis of variance (ANOVA) and the Wilcoxon nonparametric means comparison test to characterize differences among groups of years according to precipitation classification. We used multiple linear
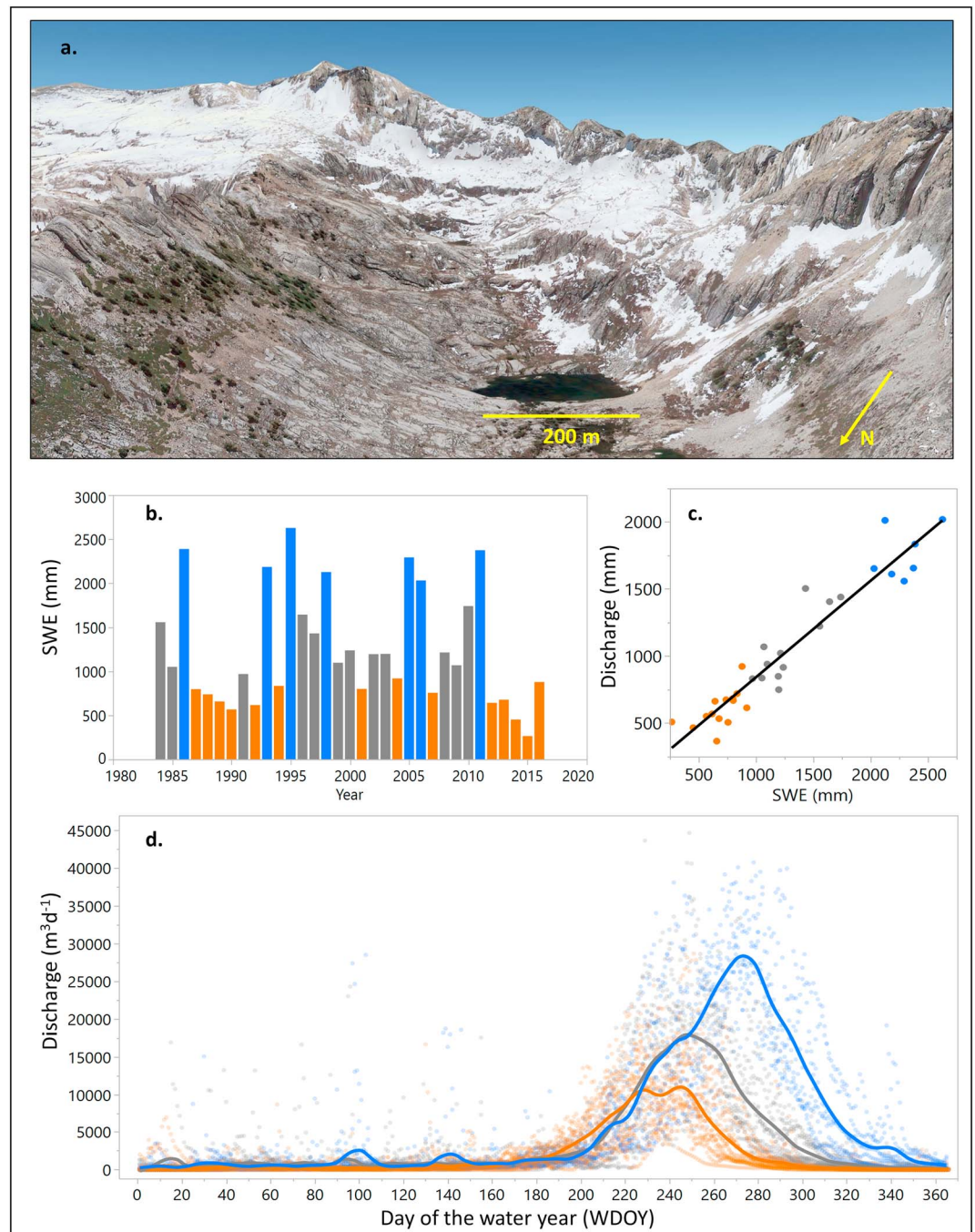
Figure 1. Hydrological variation in relation to snow in the Emerald Basin. (a) View of Emerald Lake (2.7 ha) and the basin (120 ha). (b) Basin-wide estimates of snow water equivalent (SWE) made between 1984 and 2016. (c) Relationship between SWE and total annual discharge. (d) Annual patterns in discharge (points correspond to daily Q and lines are spline fits, lambda 1,000–2,000). The day of the water year (WDOY) is the sequential day starting on 1 October. Years are color coded according to magnitude of SWE, with drought years orange (SWE < 900 mm), wet years blue (SWE > 1,700 mm), and average years gray (SWE 900–1,700 mm).

regression modeling to test for climate trends in metrics of snowmelt and lake particulate carbon and nitrogen concentrations. We tested for autocorrelation by evaluating plots of model residuals against time and found no relationship. We used pairwise correlations and principal component analysis to illustrate relationships among climate, hydrodynamic, and limnological factors and serve as the mechanistic basis in the development of general linear models. Data distributions were evaluated and found to meet necessary

Table 2

Analysis of Variance and Nonparametric Means Comparisons Illustrate Differences in Snowmelt Characteristics Among Years Classified According to SWE as Dry, Average, or Wet

	Fit statistics			Estimates			Means comparison (Wilcoxon)		
	DF	F	P	Dry (N = 14)	Average (N = 12)	Wet (N = 7)	Wet (7)	Average (12)	Dry (14)
Q	32	77.5	<0.0001	603	1066	1763	A	B	C
Start DOY	32	12.0	0.0002	173	201	197	A	A	B
50% DOY	32	40.3	<0.0001	229	245	265	A	B	C
Peak DOY	32	10.7	0.0003	234	241	265	A	B	B
End DOY	32	36.1	<0.0001	286	304	339	A	B	C
DRL	32	0.758	0.4773	81	104	80	A	A	A
DDL	32	0.802	0.458	65	77	72	A	A	A
DSM	32	8.60	0.0011	113	103	141	A	B	B
MRRL	32	7.28	0.0027	5.0	4.8	10	A	B	B
MRDL	32	22.83	<0.0001	4.3	7.4	11	A	C	B
MRSM	32	23.7	<0.0001	4.5	5.7	11	A	B	B

Note. Snowmelt characteristics that differed significantly across classification types have different letters (A, B, or C). DOY is day of the water year. Start, Peak, 50%, and End all identify the DOY on which snowmelt starts, peaks, reaches 50% cumulative discharge, and ends. The duration of melt is quantified for the entire snowmelt period (DSM) and for the rising (DRL) and descending (DDL) limbs of the hydrograph. Likewise, the rate of melt is computed for the entire snowmelt period (MRSM) and for the rising (MRRL) and descending (MRDL) of the hydrograph.

assumptions of normality. All statistical analyses were conducted using JMP version 12 (SAS Institute) and Matlab version R2017a (MathWorks).

3. Results

3.1. Climate and Variation in SWE Regulate Snowmelt

Discharge and snowmelt in the Emerald Lake basin are controlled primarily by the magnitude of winter snowpack accumulating in that water year (Figure 1). Between 1984 and 2016, SWE ranged by a factor of 10, from 265 mm to 2,628 mm (Figure 1a). Variations in SWE were associated with variations in annual discharge (Figure 1b), which spanned a factor of 5.5 across the range of SWE. Snowmelt had similar patterns across years that were classified according to magnitude of SWE as dry, average, and wet (Figure 1c).

Nearly all attributes associated with the timing, duration, and rate of melt (Table 1) varied significantly in relation to SWE and a range of other climate variables (Tables 2 and 3 and Figures 2 and 3). In general, dry years with shallower snowpack experienced an earlier onset of melt, took fewer days for melt to reach completion, and had lower MRs than wet years with larger snowpack.

Table 3

Pairwise Correlations Between Climate Variables and Characteristics of the Snowmelt Hydrograph Associated With Timing, Duration, and Rate of Melt

		SWE	SS	AT	WS	WD	RH	SWR	LWR	Outlet T
Timing	Start DOY	0.50*	0.48*	−0.51*	0.14	0.06	0.11	−0.20	−0.01	−0.73*
	Peak DOY	0.56*	0.40*	−0.70*	0.14	0.02	0.54*	0.05	−0.21*	−0.61*
	50% DOY	0.85*	0.53*	−0.76*	0.33*	0.21	0.51*	−0.03	−0.34*	−0.89*
	End DOY	0.87*	0.43*	−0.60*	0.36*	0.38*	0.41*	0.01	−0.35*	−0.84*
Duration	DRL	0.04	−0.09	−0.12	−0.03	0.04	−0.05	−0.17	0.04	−0.74*
	DDL	0.17	−0.12	0.17	0.62*	0.44*	0.18	0.20	−0.39*	−0.60*
	DSM	0.45*	0.04	−0.17	0.24*	0.34*	0.34*	0.19	−0.35*	−0.04
Rate	MRRL	0.44*	0.50*	−0.38*	0.27*	0.12	0.28*	0.09	−0.15	−0.35*
	MRDL	0.86*	0.58*	−0.56*	0.32*	0.15	0.25*	−0.11	−0.20	0.59*
	MRSM	0.74*	0.56*	−0.49*	0.31*	0.16	0.29*	0.04	−0.21*	0.43*

Note. DOY is day of the water year. Start, Peak, 50% and end all identify the DOY on which snowmelt starts, peaks, reaches 50% cumulative discharge, and ends. The duration of melt is quantified for the entire snowmelt period (DSM) and for the rising (DRL) and descending (DDL) limbs of the hydrograph. Likewise, the rate of melt is computed for the entire snowmelt period (MRSM) and for the rising (MRRL) and descending (MRDL) of the hydrograph.
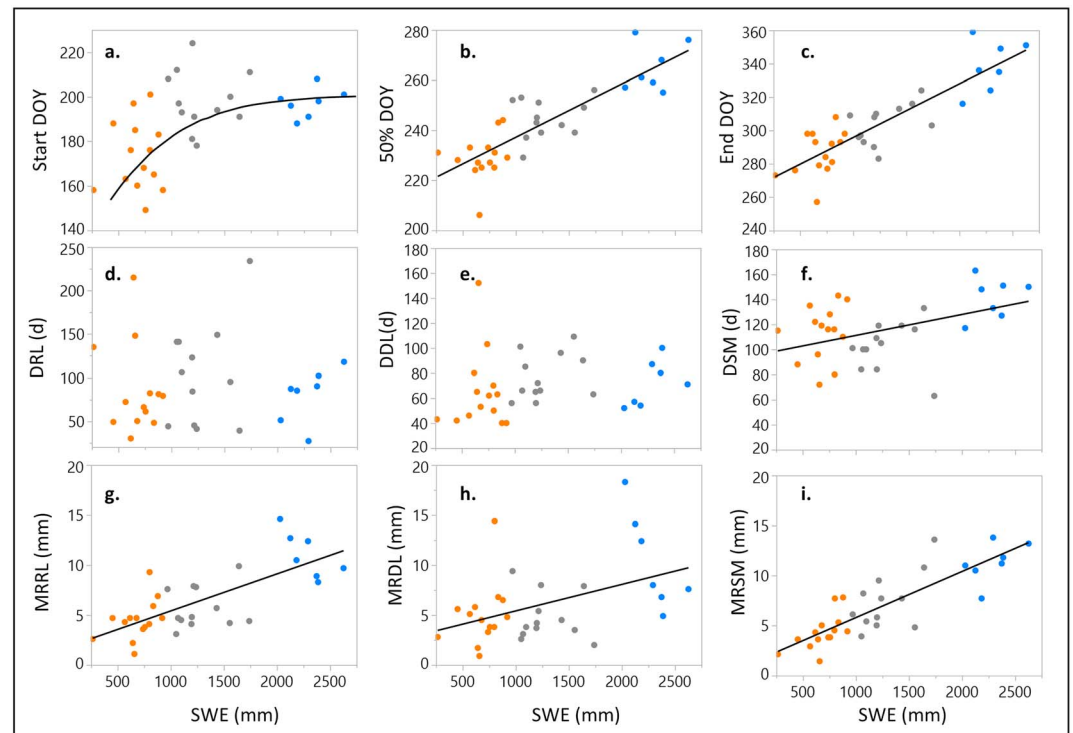*Values significant at $P < 0.05$.

Figure 2. Relationships between snowmelt characteristics and total annual snow water equivalent (SWE) across all years. SWE was the primary factor controlling variation in characteristics of the snowmelt hydrograph associated with the timing of melt (a–c), the duration of melt (d–f), and the melt rate (g–i). Snowmelt metric abbreviations correspond to Table 1. Points are color coded according to SWE as in Figure 1.

Of the three categories of snowmelt attributes, factors related to timing were most strongly regulated by SWE (Table 2 and Figures 2a–2c). The days on which snowmelt began and peaked ranged over a period of 90 days, and the day on which melt ended varied by over 100 days (Table 3).

As would be expected on the basis of the snowmelt energy budget (Jepsen et al., 2012), all attributes of timing were negatively correlated with shortwave radiation, longwave radiation, and air temperature and positively correlated with the wind speed, relative humidity, and the amount of late spring snow (Figure 3a). The correlations between air temperature and snowmelt timing were stronger for Peak DOY and 50% DOY than for Start DOY and End DOY.

Attributes related to the duration of snowmelt were less strongly correlated with SWE and more evenly related to other climate factors (Table 3). The overall duration of snowmelt did increase with increasing SWE (Table 2 and Figures 2d–2f), but there was considerable scatter in the relationship during both the rising and descending limbs of the hydrograph. The rising limb, which ranged from 16 to 234 days (Table 3), was not significantly related to any of the climate factors we tested. However, DDL and DSM were both positively correlated with wind speed and direction and negatively correlated with longwave radiation (Table 3 and Figure 3b).

While a variety of factors were correlated with aspects of MR (Table 3), correlations with SWE or amount of spring snowfall were strongest (Table 2; Figure 2 g-i; Figure 3c). More variation in MRDL was explained by SWE and spring snow than MRRL. In both cases, however, higher MRs were associated with increasing SWE and accumulation of spring snow. The rate of melt was positively correlated with Start DOY (Figure 3c), and MRs were lower in years when snowmelt started earlier in the season. Air temperature was not strongly correlated with melt during the rising limb of the hydrograph. Somewhat counterintuitively colder spring air temperatures were positively correlated with larger MRDL in years with more snow (Table 3; Figure 3c).

3.2. Intraannual Patterns in Factors Influencing Phytoplankton Biomass

By affecting spring snowmelt, SWE exerts control over lake flushing rates, water temperature, and nutrient concentrations that affect phytoplankton biomass. Seasonal rates of warming, maximum temperatures and
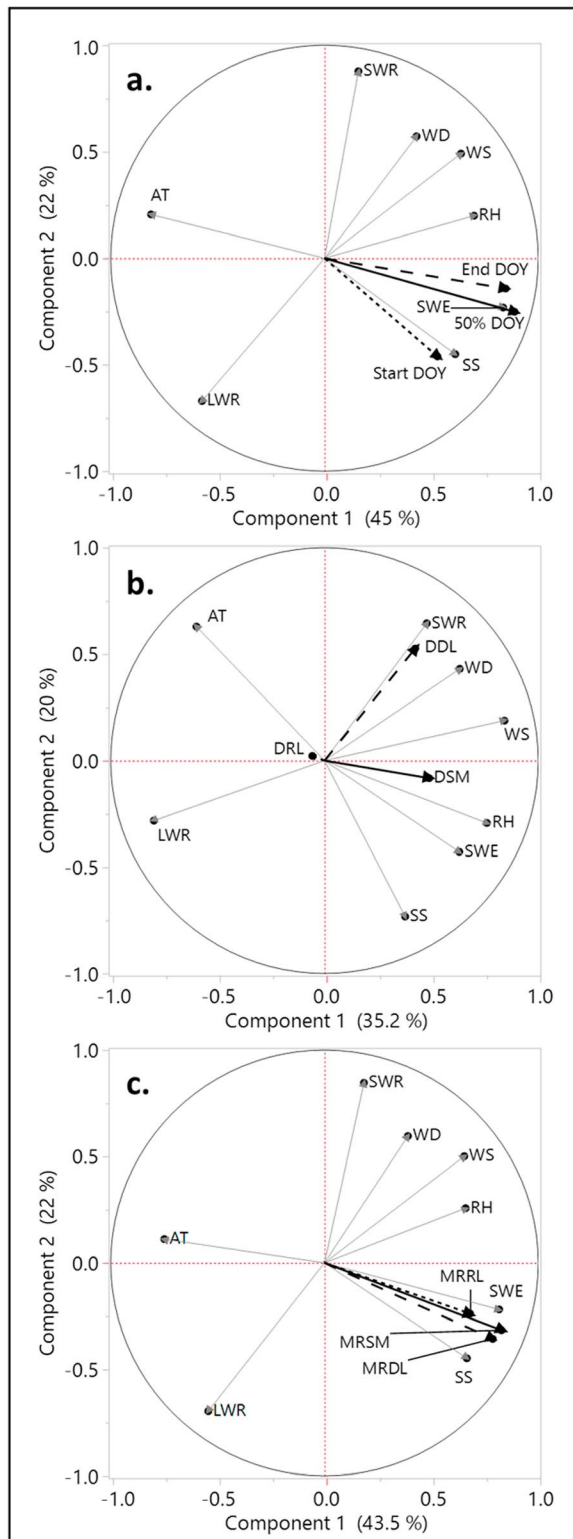
Figure 3. Results from principal component analysis for spring climate variables and snowmelt characteristics associated with timing (a), duration (b), and melt rate (c). AT = air temperature; SWR = shortwave radiation; LWR = longwave radiation; WS = wind speed; WD = wind direction; SS = spring snow; SWE = estimate of annual accumulated snow water equivalent.

duration of elevated temperature in Emerald Lake were all strongly regulated by SWE (Figure 4a). In dry years, the lake begins warming earlier and stays warm longer than in wet years. Moreover, during wet years the percent lake volume per day flushing rate was 8.2, which was twice as high as the 3.3 and 4.2 rate measured in dry and average years, respectively (ANOVA $R^2 = 0.61$; $F_{2,32} = 23.68$, $p = 0.0001$).

Seasonal variation in the timing of peak nutrient concentrations was affected by the magnitude of annual SWE. Nitrate concentrations in the lake and outflow ranged from less than 1 μM to 16 μM over the course of spring to autumn in most years (Figure 4b). Peak annual nitrate concentration and patterns of increase during snowmelt are strongly correlated to SWE (Heard & Sickman, 2016; Sickman et al., 2001; Sickman, Leydecker, Chang, et al., 2003). Nitrate consistently increased during the rising limb of the hydrograph regardless of the magnitude of SWE. Although concentrations during the rising limb of dry years were lower than wet or average years, they remained significantly higher during the summer months. In contrast, SRP concentrations were consistently below 0.1 μM (Figure 4c).

Particulate carbon and nitrogen concentrations were higher during the summer months of dry years (Figures 5a and 5b). Mean PC concentrations were 31.4 μM during dry summers, significantly higher than the 21.2 μM–23.5 μM found during average to wet years (ANOVA $R^2 = 0.51$; $F_{2,18} = 8.168$, $p = 0.0036$). Similarly, PN concentrations were 2.7 μM in dry years, ~1 μM higher than those found during average to wet years (ANOVA $R^2 = 0.37$; $F_{2,19} = 4.959$, $p = 0.0201$). In the case of both PC and PN, concentrations were largely invariant until the onset of snowmelt, after which they declined in wet years, but increased or remained elevated in dry years.

Although annual variation in the C:N molar ratio was 5–35, values typically ranged between 8 and 18 and had no variation with the magnitude of SWE (Figure 4c). C:N values were highest during spring and tended to decline over the course of the summer, when mean and standard deviation of C:N was 13.2 ± 4.4.

3.3. Multidecadal Trends in Snowmelt and POM

To explore the factors governing long-term trends in factors reflecting summer phytoplankton biomass, we conducted a principal component analysis that combined characteristics of spring melt with average summer climate conditions (Table 4). Principal Component 1 accounted for 39% of the variation among the factors and was strongly correlated with SWE (+), 50% DOY and End DOY (+), MRDL (+), and outlet temperature (−). Principal Component 2 accounted for 21.5% of variation and was strongly correlated with summer air temperature (+), wind speed (−), shortwave radiation (−), and longwave radiation (+). Nitrate concentration was weakly correlated with both PC1 (−) and PC2 (+).

Principal Components 1 and 2 were both predictors of summer particulate C and N concentrations (Figure 6). Alone, Component 1 accounted for 53% of variation in particulate carbon (Figure 6a; $F_{1,8} = 7.96$, $p = 0.0257$) and 62% of the variation in particulate N (Figure 6c; $F_{1,8} = 11.52$, $p = 0.0115$). Component 2 had a stronger effect on particulate C than Component 1, accounting for 82% of variation (Figure 6b; $F_{1,8} = 32.6$, $p = 0.0007$). However, Component 2 accounted for less variation in particulate N than Component 1, only 22%, and had a non-significant p value (Figure 6d; $F_{1,8} = 2.00$, $p = 0.2002$). A multiple
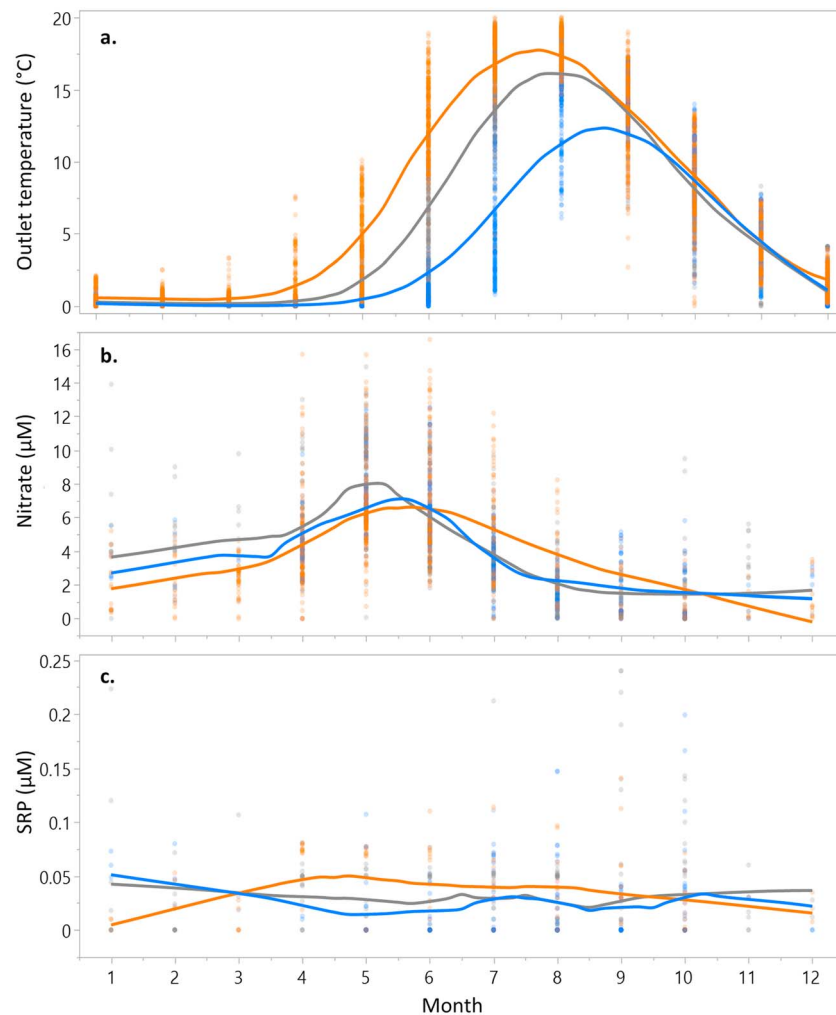
Figure 4. Monthly variation in outlet temperature (a), nitrate concentration (b), and soluble reactive phosphorus (SRP) concentration (c). Each point represents a daily value. Color codes correspond to SWE anomaly as in Figure 1.

linear regression model for particulate C combining both Components 1 and 2 accounted for 94% of variation in summer concentrations ($R^2 = 0.94$; $F_{2,8} = 44.90$, $p = 0.0002$) with standardized ß weights reflecting the stronger influence of Component 2 in the model. A similar model for particulate N ($R^2 = 0.63$; $F_{2,8} = 5.19$, $p = 0.0491$) did not account for any more variation than accounted for in a model with Component 1 alone.

We found no evidence of trends through time between 1984 and 2016 for most aspects of snowmelt (Table 5). After accounting for variation in SWE, only the descending limb of the snowmelt hydrograph showed a long-term trend. There was not a significant temporal trend in either particulate C or N (Figures 7a and 7b). However, there was a strong correlation between concentrations of particulates and SWE (Figures 7c and 7d) and the other snowmelt characteristics and climate factors associated with Principal Components 1 and 2 (Table 4). Across only years classified as dry, there were increasing trends in both particulate C ($R^2 = 0.19$; $F_{1,8} = 1.62$, $p = 0.2443$) and N ($R^2 = 0.40$; $F_{1,8} = 4.57$, $p = 0.0698$), though high variation even among the subset of dry years prevented them from being statistically significant.

4. Discussion

It is broadly accepted that the onset of snowmelt is shifting to an earlier date in mountain ecosystems across western North America, driven in part by decreasing winter snowpack, a decline in late spring snow, and a
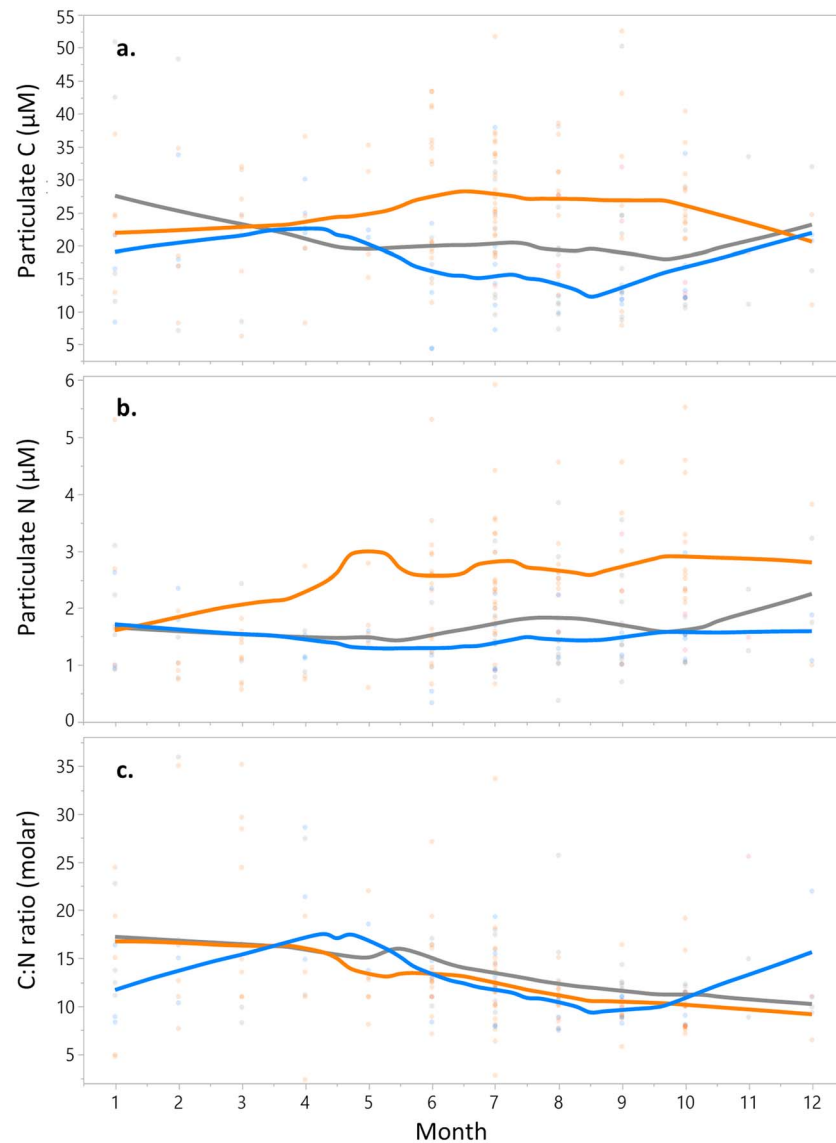
Figure 5. Monthly variation in concentration of particulate carbon (a), particulate nitrogen (b), and the C:N ratio (c). Each point represents a daily value. Color codes correspond to SWE anomaly as in Figure 1.

shift toward increased frequency of precipitation falling as rain (Lundquist et al., 2009). Empirical evidence from over 30 years of study at Emerald Lake confirm our predictions that snowmelt at higher elevation sites is more dependent on variation in the magnitude of snowpack than other long-term climate changes (Figure 1 and Tables 2 and 3), underscoring the elevation dependence of climate effects in mountains. By controlling the timing, magnitude, and duration of snowmelt (Table 2 and Figure 2), variation in SWE determines nutrient concentrations and water temperatures during the summer (Figure 4). Interactions among these factors provide bottom-up control of phytoplankton biomass and regulate POM concentrations (Figure 5). Our results suggest that climate-related effects in high-elevation ecosystems will be driven in large part by changes in the accumulation and melt of winter snow (Figure 7). As a consequence, the frequency and severity of drought is likely to have a larger impact on the ecosystem function of small, snowmelt-dominated lakes than long-term climate warming trends alone.

4.1. Variation in Climate Regulates Long-Term Trends in Snowmelt

Our study suggests that large-scale models that predict an earlier onset to snowmelt need to better account for local-scale spatial variability in mountain systems. Despite evidence that snowmelt is occurring 1 to 3

Table 4

Loading Matrix From Principal Component Analysis That Includes Factors Related to Spring Snowmelt Characteristics and Summer Climatic Conditions, All Factors Expected to Influence Lake Phytoplankton Biomass

	PC 1 (39.1%)	PC 2 (21.5%)
SWE	0.93*	0.21*
Start DOY	0.57*	0.36*
50% DOY	0.88*	0.27*
End DOY	0.92*	0.04
MRRL	0.47*	0.15
MRDL	0.84*	0.29*
Outlet temperature	−0.97*	−0.15
Nitrate	−0.24*	0.16
Air temperature	−0.47*	0.63*
Wind speed	0.36*	−0.85*
Wind direction	0.29*	−0.52*
Relative humidity	0.39*	0.07
Shortwave radiation	0.07	−0.76*
Longwave radiation	−0.39*	0.79*

Note. DOY is day of the water year. Start, Peak, 50% and end all identify the DOY on which snowmelt starts, peaks, reaches 50% cumulative discharge, and ends. The duration of melt is quantified for the entire snowmelt period (DSM) and for the rising (DRL) and descending (DDL) limbs of the hydrograph. Likewise, the rate of melt is computed for the entire snowmelt period (MRSM) and for the rising (MRRL) and descending (MRDL) of the hydrograph.
*Values significant at $P < 0.05$.

weeks earlier in mountain catchments of western North America (Regonda et al., 2005; Stewart et al., 2004, 2005), we found no statistically significant change in the day on which snowmelt begins, reaches 50% melt, or ends across all years. We did, however, find patterns of change occurring during drought years that are consistent with other studies.

This discrepancy is perhaps not surprising when we consider that most modeling and empirical studies of snowmelt have focused on larger catchments that include more area at lower elevations. Because lower-elevation sites usually accumulate less snow than higher-elevation sites, the regulatory strength of SWE with respect to other climate factors is reduced. Consequently, we would expect high-elevation catchments to behave more like low-elevation catchments during dry years, as our data demonstrate. For example, although considerable variation in Start DOY was explained across the entire range of SWE in the Emerald catchment, during dry years SWE alone had little explanatory power. When other climate factors are included in the model, nearly all the variation in Start DOY was explained ($R^2 = 0.99, F_{1,6} = 181092.6; P = 0.0018$) and standardized ß values reflect comparatively equal effects of SWE, spring snow, wind, and longwave radiation. Moreover, although there was no evidence for long-term trends across all years, there was a significant trend among dry years alone. The onset of snowmelt has shifted 23 days earlier in dry years ($R^2 = 0.54, F_{1,9} = 9.2475; P = 0.0160$; Start DOY = 1613.8−0.72 years) excluding four dry years with larger than average amounts of late spring precipitation (2001, 2012, 2014, and 2016). These results emphasize the variable role of different climate factors in regulating snowmelt at small spatial scales within mountain systems.

The earlier onset of melt during dry years corresponded with slower MRs during both the rising and descending limbs of the snowmelt hydrograph (Figures 2g and 2h and Table 1). This is consistent with expectations that shallower snowpacks in dry years begin melting earlier when energy inputs are lower (Jepsen et al., 2012; Musselman et al., 2017; Trujillo & Molotch, 2014), resulting in slower MRs. The slower MRs observed during
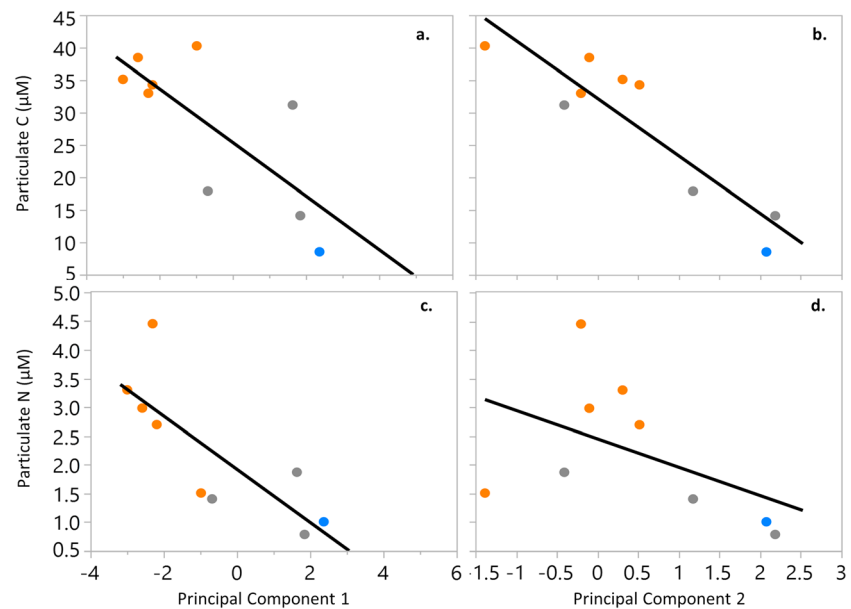

Figure 6. Relationships between principal components associated with spring snowmelt dynamics, summer climatological attributes and lake temperature (Table 3), and concentrations of particulate carbon (a and b) and nitrogen (b and c). Color codes correspond to SWE anomaly as described in Figure 1 caption.

Table 5
Multiple Regression Models Were Used to Test for Trends Through Time in Snowmelt Characteristics and Biogeochemical Particulate Carbon (C) and Nitrogen (N) Concentrations, Which Serve as Proxies for Phytoplankton Biomass in Emerald Lake

	N	RMSE	Rsq	Rsq Adj	F Ratio	Prob > F	Intercept			SWE			Year		
							Estimate	t Ratio	Prob > t	Estimate	t Ratio	Prob > t	Estimate	t Ratio	Prob > t
Start DOY	33	15.9	0.26	0.21	5.36	0.010	261	0.440	0.6604	0.014	3.22	0.0031	−0.05	−0.16	0.878
Peak DOY	33	15.5	0.33	0.29	7.52	0.002	−317	−0.550	0.5839	0.017	3.85	0.0006	0.27	0.94	0.353
50% DOY	33	8.8	0.72	0.71	39.5	<.0001	−54	−0.170	0.8693	0.022	8.88	<.0001	0.13	0.83	0.413
End DOY	33	11.7	0.77	0.76	51.2	<.0001	822	1.90	0.0665	0.032	9.78	<.0001	−0.28	−1.3	0.206
DRL	33	52.4	0.01	−0.05	0.207	0.814	−1084	−0.560	0.5795	0.004	0.300	0.7674	0.58	0.60	0.550
DDL	33	20.4	0.34	0.30	7.72	0.002	2895	3.84	0.0006	0.004	0.640	0.5251	−1.41	−3.8	0.001
DSM	33	21.8	0.22	0.17	4.31	0.023	779	0.970	0.3417	0.016	2.67	0.012	−0.34	−0.85	0.403
MRRL	33	3.6	0.20	0.14	3.7	0.038	−53	−0.40	0.6941	0.003	2.7	0.0111	0.03	0.4	0.679
MRDL	33	1.6	0.80	0.79	60.8	<.0001	−188	−3.18	0.0034	0.005	10.88	<.0001	0.09	3.2	0.003
MRSM	33	2.2	0.56	0.53	19.38	<.0001	−96	−1.170	0.2501	0.004	6.21	<.0001	0.05	1.19	0.242
Particulate C	19	7.2	0.47	0.40	7.05	0.006	202	0.64	0.5303	−0.010	−3.73	0.0018	−0.08	−0.5	0.607
Particulate N	20	0.8	0.33	0.25	4.19	0.033	−2	−0.050	0.959	−0.001	−2.73	0.0142	0.00	0.14	0.888

Note. Values in black are significant (P < 0.05) and those in gray were not significant.

dry years also explains why there was little variation in the duration of melt during the rising limb of the hydrograph. Although there is less snow to melt in dry years and snowmelt begins earlier, the slower MR means that the overall duration is similar to wet years, which begin melting later but melt faster. This explanation might also account for the lack of variation in the fraction of snowmelt occurring during late spring and early summer across years with different SWE, despite evidence for declines of up to 25% in other systems (Lundquist et al., 2009; Stewart et al., 2005).

4.2. Mechanisms Linking Variation in SWE to Phytoplankton Biomass and Implications for Mountain Lakes

POM concentrations in Emerald Lake, reflective of phytoplankton biomass, were strongly regulated by SWE. This result is consistent with studies from other mountain lakes, where increases in algal productivity are associated with changes in climate (Miller & McKnight, 2015; Park et al., 2004; Preston et al., 2016; Strub et al., 1985). Our study provides insight into the mechanisms involved. The patterns we observe suggest that changes in biomass are associated with interactions between precipitation patterns, snowmelt including timing and rates of melt, nutrient concentrations, and water temperature (Table 3). Most of these factors were either directly or indirectly regulated by SWE, which is why it had so much explanatory power over summer POM concentrations.

Perhaps most importantly, SWE controls the duration of snow and ice cover, which regulate the timing of light availability and the length of the growing season. Sierran lakes can spend up to 9 months under ice and snow, and the timing of ice-off is correlated with the magnitude of annual SWE. Because lake ice in the Sierra is made up of a composite of thin ice lenses and bands of slush and snow, little to no light reaches the lake until ice-off. In addition, SWE regulates a number of aspects of snowmelt and catchment biogeochemical processes important to phytoplankton. Flushing rates can affect the biomass of phytoplankton displaced from lakes during snowmelt (Sadro & Melack, 2012). Moreover, MRs may affect the extent to which lakes mix completely in the spring (Cortés et al., 2017; Kirillin, 2010; Kirillin et al., 2012), with important implications for both the supply of nutrients from the hypolimnion (Jassby et al., 1990) and the mixing into the epilimnion and retention of phytoplankton cells trapped in the hypolimnion over the winter. MRs also affect the timing and magnitude of nutrient delivery by affecting biogeochemical cycling and retention in catchment soils (Sickman, Leydecker, Chang, et al., 2003; Sickman et al., 2001). Finally, by directing seasonal flushing rates and duration of ice cover, SWE regulates summer rates of warming and maximum temperatures in lakes (Jassby et al., 1990).

Snowmelt in Emerald Lake appears to regulate summer phytoplankton biomass by establishing conditions favorable for primary productivity at the start of the summer. Although peak nitrate concentrations are larger in wet years, concentrations at the start of summer are higher in dry years because dilution from flushing during the descending limb of the snowmelt hydrograph is lower (Sickman, Leydecker, Chang, et al., 2003). Lake temperatures at the start of summer are correspondingly warmer. As a consequence, conditions supporting the accumulation of phytoplankton biomass are more favorable during dry years. In wet years, higher flushing rates reduce phytoplankton biomass within the lake, snowmelt dilution reduces nitrate concentrations at the start of summer (Figure 4), and longer periods of ice cover and larger volumes of cold inflowing melt waters reduce light levels and suppress temperatures. These mechanisms are consistent across a number of different mountain sites (Miller & McKnight, 2015; Park et al., 2004; Parker et al., 2008; Preston et al., 2016).

Unlike some mountain lakes, we found no biomass carryover effect between successive years. For example, in subalpine Castle Lake phytoplankton biomass and productivity were strongly correlated between years (Goldman et al., 1989; Jassby et al., 1990).
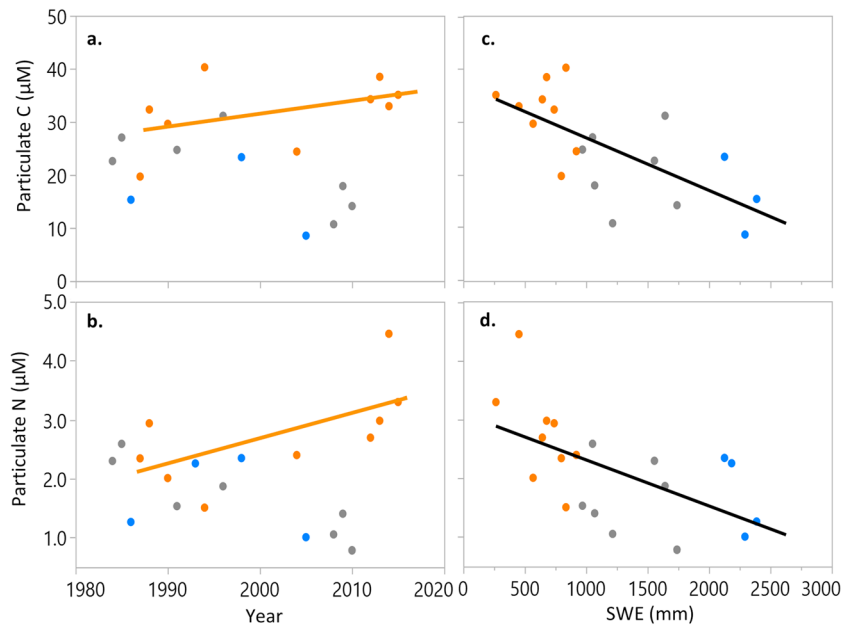
Figure 7. Mean summer concentrations of particulate carbon (a and c) and particulate nitrogen (b and d) from 1984 to 2016 plotted through time and along a gradient in SWE. Color codes correspond to SWE anomaly as described in Figure 1 caption. Orange regression line in (a) and (b) corresponds to the relationship found only in years classified as dry.

An increase in nutrients in the otherwise oligotrophic epilimnion following years with high productivity was theorized as the mechanism (Elser et al., 1995; Park et al., 2004). The lack of an effect in similarly oligotrophic Emerald Lake suggests that flushing rate plays an important role in mediating such legacy effects. Emerald Lake is both smaller and shallower than Castle Lake, often flushing with a volume of melt water 2–3 times larger than lake volume. Castle lake is both deeper and has less snow accumulation in the catchment, and incomplete or reduced periods of mixing during the spring occur (Jassby et al., 1990). It is possible that legacy effects may become more apparent in Emerald Lake during successive extreme drought years if a shift toward incomplete flushing during the spring occurs.

Our analysis focuses on bottom-up control of phytoplankton biomass (i.e., regulation through hydrology, temperature, and nutrients). Top-down control of phytoplankton by large-bodied herbivorous zooplankton, which have high phytoplankton clearance rates, is also an important mechanism in Sierra lakes without fish (Sarnelle, 1997; Sarnelle & Knapp, 2005). However, it is unlikely to be as large a factor in Emerald Lake, where the presence of nonnative trout for over half a century has altered zooplankton community structure by reducing the abundance of large-bodied grazers (Engle & Melack, 1995). The zooplankton community in Emerald Lake is dominated by rotifers in all seasons, with the mean total density of rotifers over 8 times the mean density of crustaceans. The summertime mean abundance of the most common large-bodied crustacean grazer *Daphnia* sp. was 3.2% (345 m^{-3}) of total zooplankton density in recent years. Moreover, long-term studies of other alpine systems suggest that even in lakes without fish, bottom-up effects controlled by climate exert greater control on ecosystem responses than trophic dynamics (Parker et al., 2008).

Predicting long-term climate responses in mountain lakes will require an understanding of interactions and feedbacks among drivers and how such processes may vary in space or time. For example, productivity in mountain lakes might be further amplified through positive feedbacks associated with ongoing changes. We found dry years to result in higher POM concentrations (Figure 7) as well as elevated dissolved organic carbon concentrations ($R^2 = 0.36$, $F_{1,9} = 5.125$; $P = 0.0499$). Such changes reduce water clarity and increase absorption of solar radiation contributing to increased warming that may further stimulate productivity (Fee et al., 1996; Rose et al., 2016). Small changes in water clarity might also release phytoplankton from photoinhibition (Sickman & Melack, 1992) and further increase productivity by suppressing the inhibitory effect of UV-B on phytoplankton (Williamson et al., 2010). Long-term changes in precipitation coupled with warming air temperatures are resulting in catchment level changes in weathering and nutrient cycling.

The magnitude and rate of spring snowmelt is declining at some elevations, though higher elevation sites may prove to be more resistant depending on long-term changes in drought frequency. How such changes interact to affect the loading of inorganic nutrients and organic matter will be an important determinant of how aquatic ecosystems continue to change.

Regional changes in response to altered climate are evident throughout California, many of which may indirectly affect aquatic ecosystem function. Interactions between climate warming and precipitation (Portmann et al., 2009) have contributed to increased drought frequency and severity (Diffenbaugh et al., 2015; Griffin & Anchukaitis, 2014; Williams et al., 2015), affecting soil moisture (Harpold & Molotch, 2015) and resulting in unprecedented mortality among trees (Asner et al., 2016). High-standing fuel loads and extreme fire conditions have resulted in more frequent and larger fires (Dennison et al., 2014). Soil erosion from recent burn areas or drought-denuded hillslopes is higher and may be amplified by more precipitation falling as rain rather than snow (Mote, 2003) and an increase in the frequency of extreme weather events (Melillo et al., 2014). The resulting increased loading of nutrients and terrestrial organic matter into streams and lakes will further alter the productivity and algal biomass of aquatic ecosystems (Sadro & Melack, 2012). Predicting how aquatic ecosystems will respond to climate change requires an understanding of how precipitation patterns are changing and how such changes interact with other climate and landscape level factors across a range of time scales to drive lake responses. Long-term empirical studies that capture variability across these time scales will be vital for developing such an understanding.

References

Adrian, R., O'Reilly, C. M., Zagarese, H., Baines, S. B., Hessen, D. O., Keller, W., et al. (2009). Lakes as sentinels of climate change. *Limnology and Oceanography*, *54*(6part2), 2283–2297. https://doi.org/10.4319/lo.2009.54.6_part_2.2283

Asner, G. P., Brodrick, P. G., Anderson, C. B., Vaughn, N., Knapp, D. E., & Martin, R. E. (2016). Progressive forest canopy water loss during the 2012–2015 California drought. *Proceedings of the National Academy of Sciences*, *113*(2), E249–E255. https://doi.org/10.1073/pnas.1523397113

Carpenter, S. R., Fisher, S. G., Grimm, N. B., & Kitchell, J. F. (1992). Global change and freshwater ecosystems. *Annual Review of Ecology and Systematics*, *23*(1), 119–139. https://doi.org/10.1146/annurev.es.23.110192.001003

Cayan, D. R., Kammerdiener, S. A., Dettinger, M. D., Caprio, J. M., & Peterson, D. H. (2001). Changes in the onset of spring in the western United States. *Bulletin of the American Meteorological Society*, *82*(3), 399–415. https://doi.org/10.1175/1520-0477(2001)082<0399:CITOOS>2.3.CO;2

Cortés, A., MacIntyre, S., & Sadro, S. (2017). Flowpath and retention of snowmelt in an ice-covered Arctic Lake: Flowpath and retention of snowmelt. *Limnology and Oceanography*, *62*(5), 2023–2044. https://doi.org/10.1002/lno.10549

Dennison, P. E., Brewer, S. C., Arnold, J. D., & Moritz, M. A. (2014). Large wildfire trends in the western United States, 1984–2011. *Geophysical Research Letters*, *41*, 2928–2933. https://doi.org/10.1002/2014GL059576

Diffenbaugh, N. S., Swain, D. L., & Touma, D. (2015). Anthropogenic warming has increased drought risk in California. *Proceedings of the National Academy of Sciences*, *112*(13), 3931–3936. https://doi.org/10.1073/pnas.1422385112

Elser, J. J., Lubnow, F. S., Marzolf, E. R., Brett, M. T., Dion, G., & Goldman, C. R. (1995). Factors associated with interannual and intraannual variation in nutrient limitation of phytoplankton growth in Castle Lake, California. *Canadian Journal of Fisheries and Aquatic Sciences*, *52*(1), 93–104. https://doi.org/10.1139/f95-009

Engle, D., & Melack, J. M. (1995). Zooplankton of high-elevation lakes of the Sierra-Nevada, California—Potential effects of chronic and episodic acidification. *Archiv für Hydrobiologie*, *133*, 1–21.

Fee, E. J. (1980). Important factors for estimating annual phytoplankton production in the experimental lakes area. *Canadian Journal of Fisheries and Aquatic Sciences*, *37*(3), 513–522. https://doi.org/10.1139/f80-066

Fee, E. J., Hecky, R. E., Kasian, S. E. M., & Cruikshank, D. R. (1996). Effects of lake size, water clarity, and climatic variability on mixing depths in Canadian Shield lakes. *Limnology and Oceanography*, *41*(5), 912–920. https://doi.org/10.4319/lo.1996.41.5.0912

Fountain, A. G., Campbell, J. L., Schuur, E. A. G., Stammerjohn, S. E., Williams, M. W., & Ducklow, H. W. (2012). The disappearing cryosphere: Impacts and ecosystem responses to rapid cryosphere loss. *BioScience*, *62*(4), 405–415. https://doi.org/10.1525/bio.2012.62.4.11

Goldman, C. R., Jassby, A., & Powell, T. (1989). Interannual fluctuations in primary production—Meteorological forcing at 2 subalpine lakes. *Limnology and Oceanography*, *34*(2), 310–323. https://doi.org/10.4319/lo.1989.34.2.0310

Greig, H. S., Kratina, P., Thompson, P. L., Palen, W. J., Richardson, J. S., & Shurin, J. B. (2012). Warming, eutrophication, and predator loss amplify subsidies between aquatic and terrestrial ecosystems. *Global Change Biology*, *18*(2), 504–514. https://doi.org/10.1111/j.1365-2486.2011.02540.x

Griffin, D., & Anchukaitis, K. J. (2014). How unusual is the 2012–2014 California drought? *Geophysical Research Letters*, *41*, 9017–9023. https://doi.org/10.1002/2014GL062433

Harpold, A. A., & Molotch, N. P. (2015). Sensitivity of soil water availability to changing snowmelt timing in the western U.S.: Soil moisture and changing snowmelt. *Geophysical Research Letters*, *42*, 8011–8020. https://doi.org/10.1002/2015GL065855

Heard, A. M., & Sickman, J. O. (2016). Nitrogen assessment points: Development and application to high-elevation lakes in the Sierra Nevada, California. *Ecosphere*, *7*(11), e01586. https://doi.org/10.1002/ecs2.1586

Herschy, R. W. (Ed) (1978). *Hydrometry: Principles and practices, Chichester [Eng.]*. New York: John Wiley.

Jassby, A. D., Powell, T. M., & Goldman, C. R. (1990). Interannual fluctuations in primary production: Direct physical effects and the trohic cascade at Castle Lake, California. *Limnology and Oceanography*, *35*(5), 1021–1038. https://doi.org/10.4319/lo.1990.35.5.1021

Jepsen, S. M., Molotch, N. P., Williams, M. W., Rittger, K. E., & Sickman, J. O. (2012). Interannual variability of snowmelt in the Sierra Nevada and Rocky Mountains, United States: Examples from two alpine watersheds. *Water Resources Research*, *48*, W02529. https://doi.org/10.1029/2011WR011006

Jones, H. G. (Ed) (2001). *Snow ecology: An interdisciplinary examination of snow-covered ecosystems*. Cambridge, UK; New York, NY: Cambridge University Press.

Kattelmann, R., & Elder, K. (1991). Hydrologic characteristics and water-balance of an alpine basin in the Sierra-Nevada. *Water Resources Research*, *27*, 1553–1562. https://doi.org/10.1029/90WR02771

Kilpatrick, F. A., & Cobb, E. D. (1987). Measurement of discharge using tracers: U.S. Geological Survey techniques of water-resource investigations. US Government Printing Office.

Kirillin, G. (2010). Modeling the impact of global warming on water temperature and seasonal mixing regimes in small temperate lakes. *Boreal Environment Research*, *15*, 279–293.

Kirillin, G., Leppäranta, M., Terzhevik, A., Granin, N., Bernhardt, J., Engelhardt, C., et al. (2012). Physics of seasonally ice-covered lakes: A review. *Aquatic Sciences*, *74*(4), 659–682. https://doi.org/10.1007/s00027-012-0279-y

Leydecker, A., & Melack, J. M. (2000). Estimating evaporation in seasonally snow-covered catchments in the Sierra Nevada, California. *Journal of Hydrology*, *236*, 121–138. https://doi.org/10.1016/S0022-1694(00)00290-0

Leydecker, A., Sickman, J. O., & Melack, J. M. (2001). Spatial scaling of hydrological and biogeochemical aspects of high-altitude catchments in the Sierra Nevada, California, USA. *Arctic Antarctic and Alpine Research*, *33*(4), 391–396. https://doi.org/10.2307/1552547

Lundquist, J. D., Cayan, D. R., & Dettinger, M. D. (2004). Spring onset in the Sierra Nevada: When is snowmelt independent of elevation? *Journal of Hydrometeorology*, *5*(2), 327–342. https://doi.org/10.1175/1525-7541(2004)005<0327:SOITSN>2.0.CO;2

Lundquist, J. D., Dettinger, M. D., & Cayan, D. R. (2005). Snow-fed streamflow timing at different basin scales: Case study of the Tuolumne River above Hetch Hetchy, Yosemite, California. *Water Resources Research*, *41*, W07005. https://doi.org/10.1029/2004WR003933

Lundquist, J. D., Dettinger, M. D., Stewart, I. T., & Cayan, D. R. (2009). Variability and trends in spring runoff in the western United States. In *Climate Warming in Western North America: Evidence and Environmental Effects* (Chapter 5, p. 63–76). Salt Lake City, Utah: University of Utah Press.

Maurer, E. P., Stewart, I. T., Bonfils, C., Duffy, P. B., & Cayan, D. (2007). Detection, attribution, and sensitivity of trends toward earlier streamflow in the Sierra Nevada. *Journal of Geophysical Research*, *112*, D11118. https://doi.org/10.1029/2006JD008088

Melack, J. M., & Stoddard, J. L. (1991). Sierra Nevada, California. In D. F. Charles (Ed.), *Acidic deposition and aquatic ecosystems*, (pp. 503–530). New York: Springer. https://doi.org/10.1007/978-1-4613-9038-1_21

Melillo, J., Richmond, T., & Yohe, G. (2014). Climate change impacts in the United States: The third national climate assessment. doi:https://doi.org/10.7930/J0Z31WJ2

Miller, M. P., & McKnight, D. M. (2015). Limnology of the Green Lakes Valley: Phytoplankton ecology and dissolved organic matter biogeochemistry at a long-term ecological research site. *Plant Ecology and Diversity*, *8*(5–6), 689–702. https://doi.org/10.1080/17550874.2012.738255

Mote, P. W. (2003). Trends in snow water equivalent in the Pacific Northwest and their climatic causes. *Geophysical Research Letters*, *30*(12), 1601, https://doi.org/10.1029/2003GL017258.

Musselman, K. N., Clark, M. P., Liu, C., Ikeda, K., & Rasmussen, R. (2017). Slower snowmelt in a warmer world. *Nature Climate Change*, *7*(3), 214–219. https://doi.org/10.1038/nclimate3225

Park, S., Brett, M. T., Müller-Solger, A., & Goldman, C. R. (2004). Climatic forcing and primary productivity in a subalpine lake: Interannual variability as a natural experiment. *Limnology and Oceanography*, *49*(2), 614–619. https://doi.org/10.4319/lo.2004.49.2.0614

Parker, B. R., Vinebrooke, R. D., & Schindler, D. W. (2008). Recent climate extremes alter alpine lake ecosystems. *Proceedings of the National Academy of Sciences*, *105*(35), 12,927–12,931. https://doi.org/10.1073/pnas.0806481105

Pepin, N., Bradley, R. S., Diaz, H. F., Baraer, M., Caceres, E. B., Forsythe, N., et al. (2015). Elevation-dependent warming in mountain regions of the world. *Nature Climate Change*, *5*(5), 424–430.

Pepin, N. C., & Lundquist, J. D. (2008). Temperature trends at high elevations: Patterns across the globe. *Geophysical Research Letters*, *35*, L14701. https://doi.org/10.1029/2008GL034026

Portmann, R. W., Solomon, S., & Hegerl, G. C. (2009). Spatial and seasonal patterns in climate change, temperatures, and precipitation across the United States. *Proceedings of the National Academy of Sciences*, *106*(18), 7324–7329. https://doi.org/10.1073/pnas.0808533106

Preston, D. L., Caine, N., McKnight, D. M., Williams, M. W., Hell, K., Miller, M. P., et al. (2016). Climate regulates alpine lake ice cover phenology and aquatic ecosystem structure: Climate and alpine lakes. *Geophysical Research Letters*, *43*, 5353–5360. https://doi.org/10.1002/2016GL069036

Regonda, S. K., Rajagopalan, B., Clark, M., & Pitlick, J. (2005). Seasonal cycle shifts in hydroclimatology over the western United States. *Journal of Climate*, *18*(2), 372–384. https://doi.org/10.1175/JCLI-3272.1

Roberts, J. J., Fausch, K. D., Schmidt, T. S., & Walters, D. M. (2017). Thermal regimes of Rocky Mountain lakes warm with climate change. *PLoS ONE*, *12*(7), e0179498. https://doi.org/10.1371/journal.pone.0179498

Rose, K. C., Winslow, L. A., Read, J. S., & Hansen, G. J. A. (2016). Climate-induced warming of lakes can be either amplified or suppressed by trends in water clarity: Clarity-climate warming of lakes. *Limnology and Oceanography Letters*, *1*(1), 44–53. https://doi.org/10.1002/lol2.10027

Sadro, S., & Melack, J. M. (2012). The effect of an extreme rain event on the biogeochemistry and ecosystem metabolism of an oligotrophic high-elevation lake. *Arctic, Antarctic, and Alpine Research*, *44*(2), 222–231. https://doi.org/10.1657/1938-4246-44.2.222

Sadro, S., Melack, J. M., & MacIntyre, S. (2011). Spatial and temporal variability in the ecosystem metabolism of a high-elevation lake: Integrating benthic and pelagic habitats. *Ecosystems*, *14*(7), 1123–1140. https://doi.org/10.1007/s10021-011-9471-5

Sarnelle, O. (1997). Daphnia effects on microzooplankton: Comparisons of enclosure and whole-lake responses. *Ecology*, *78*(3), 913–928.

Sarnelle, O., & Knapp, R. A. (2005). Nutrient recycling by fish versus zooplankton grazing as drivers of the trophic cascade in alpine lakes. *Limnology and Oceanography*, *50*(6), 2032–2042. https://doi.org/10.4319/lo.2005.50.6.2032

Sebestyen, S. D., Boyer, E. W., Shanley, J. B., Kendall, C., Doctor, D. H., Aiken, G. R., & Ohte, N. (2008). Sources, transformations, and hydrological processes that control stream nitrate and dissolved organic matter concentrations during snowmelt in an upland forest. *Water Resources Research*, *44*, W12410. https://doi.org/10.1029/2008WR006983

Sickman, J. O., Leydecker, A., & Melack, J. M. (2001). Nitrogen mass balances and abiotic controls on N retention and yield in high-elevation catchments of the Sierra Nevada, California, United States. *Water Resources Research*, *37*, 1445–1461. https://doi.org/10.1029/2000WR900371

Sickman, J. O., Leydecker, A. L., Chang, C. C., Kendall, C., Melack, J. M., Lucero, D. M., & Schimel, J. (2003). Mechanisms underlying export of N from high-elevation catchments during seasonal transitions. *Biogeochemistry*, *64*(1), 1–24. https://doi.org/10.1023/A:1024928317057

Sickman, J. O., & Melack, J. M. (1992). Photosynthetic activity of phytoplankton in a high altitude lake (Emerald Lake, Sierra Nevada, California). *Hydrobiologia*, *230*(1), 37–48. https://doi.org/10.1007/BF00015113

Sickman, J. O., Melack, J. M., & Clow, D. W. (2003). Evidence for nutrient enrichment of high-elevation lakes in the Sierra Nevada, California. *Limnology and Oceanography*, *48*(5), 1885–1892. https://doi.org/10.4319/lo.2003.48.5.1885

Stewart, I. T., Cayan, D. R., & Dettinger, M. D. (2004). Changes in snowmelt runoff timing in western North America under a "business as usual" climate change scenario. *Climatic Change*, *62*(1-3), 217–232. https://doi.org/10.1023/B:CLIM.0000013702.22656.e8

Stewart, I. T., Cayan, D. R., & Dettinger, M. D. (2005). Changes toward earlier streamflow timing across western North America. *Journal of Climate*, *18*(8), 1136–1155. https://doi.org/10.1175/JCLI3321.1

Strub, P. T., Powell, T., & Goldman, C. R. (1985). Climatic forcing—Effects of El Nino on a small, temperate lake. *Science*, *227*(4682), 55–57. https://doi.org/10.1126/science.227.4682.55

Trujillo, E., & Molotch, N. P. (2014). Snowpack regimes of the Western United States. *Water Resources Research*, *50*, 5611–5623. https://doi.org/10.1002/2013WR014753

Wang, Q., Fan, X., & Wang, M. (2014). Recent warming amplification over high elevation regions across the globe. *Climate Dynamics*, *43*(1–2), 87–101. https://doi.org/10.1007/s00382-013-1889-3

Williams, A. P., Seager, R., Abatzoglou, J. T., Cook, B. I., Smerdon, J. E., & Cook, E. R. (2015). Contribution of anthropogenic warming to California drought during 2012–2014. *Geophysical Research Letters*, *42*, 6819–6828. https://doi.org/10.1002/2015GL064924

Williamson, C. E., Salm, C., Cooke, S. L., & Saros, J. E. (2010). How do UV radiation, temperature, and zooplankton influence the dynamics of alpine phytoplankton communities? *Hydrobiologia*, *648*(1), 73–81. https://doi.org/10.1007/s10750-010-0147-5

Yvon-Durocher, G., Jones, J. I., Trimmer, M., Woodward, G., & Montoya, J. M. (2010). Warming alters the metabolic balance of ecosystems. *Philosophical Transactions of the Royal Society, B: Biological Sciences*, *365*(1549), 2117–2126. https://doi.org/10.1098/rstb.2010.0038